IL NUOVO CIMENTO **48 C** (2025) 5
DOI 10.1393/ncc/i2025-25005-6

Colloquia: WPCF-Resonance 2023

Wigner density approach to quarkonium production in high energy *pp* collisions

Jiaxing Zhao(1), Pol Bernard Gossiaux(1), Taesoo Song(2), Elena Bratkovskaya(2)(3)(4) and Joerg Aichelin(1)

(1) *SUBATECH UMR 6457 (IMT Atlantique, Université de Nantes, IN2P3/CNRS) 4 Rue Alfred Kastler, F-44307 Nantes, France*
(2) *GSI Helmholtzzentrum für Schwerionenforschung GmbH - Planckstrasse 1, 64291 Darmstadt, Germany*
(3) *Institute for Theoretical Physics, Johann Wolfgang Goethe Universität - Frankfurt am Main, Germany*
(4) *Helmholtz Research Academy Hesse for FAIR (HFHF), GSI Helmholtz Center for Heavy Ion Physics, Campus Frankfurt - 60438 Frankfurt, Germany*

received 23 July 2024

Summary. — The production of charmonium and bottomonium states in *pp* collisions is studied using the Wigner density formalism. For practical purposed the Wigner density of the quarkonia is approximated by analytical 3-D isotropic harmonic oscillator Wigner densities with the same root-mean-square radius as the wave function, which is given by the solution of the Schrödinger equation. This approach reproduces quite well the available experimental transverse momentum and rapidity distributions.

1. – Introduction

Hidden heavy flavor mesons serve as valuable tool for studying the strongly interacting quark gluon plasma (QGP), which forms during high-energy heavy-ion collisions. Due to the large quark mass m_Q, where $m_Q \gg \Lambda_{\rm QCD}$, with $\Lambda_{\rm QCD}$ representing the QCD cutoff, the production of quarkonium can be factorized into two main processes. Firstly, the production of a heavy quark pair $Q\bar{Q}$, which can be described by perturbative QCD. Secondly, a subsequent soft non-perturbative process describes the formation of a colorless quarkonium state from the $Q\bar{Q}$ pair. Various approaches have been proposed for this latter process, including the Color-Evaporation Model (CEM), the Color-Singlet Model (CSM), and the Color-Octet Model (COM), with the latter two being encompassed in the Non-Relativistic QCD (NRQCD) framework. For a comprehensive review, see [1].

Recently, the rapidity and transverse momentum (p_T) distributions of hidden heavy flavor mesons, produced in proton-proton (*pp*) collisions, have been successfully reproduced using the Wigner density matrix formalism [2-4]. Here, we aim to extend this formalism up to the $3S$ state and utilize the EPOS4 model to generate the initial heavy quarks.

TABLE I. – *The masses, root-mean-square radii, and the Gaussian widths σ of different charmonium and bottomonium states in vacuum. The experimental data are from ref.* [7].

	J/ψ	$\chi_c(1P)$	$\psi(2S)$	$\Upsilon(1S)$	$\chi_b(1P)$	$\chi_b(1D)$	$\Upsilon(2S)$	$\chi_b(2P)$	$\Upsilon(3S)$
Mass Theo.(GeV)	3.071	3.483	3.652	9.390	9.870	10.109	9.959	10.208	10.288
Mass Exp. (GeV)	3.097	3.463	3.686	9.460	9.876	10.163	10.023	10.243	10.355
$\langle r^2\rangle$ (fm^2)	0.182	0.453	0.714	0.042	0.153	0.284	0.236	0.410	0.520
σ(fm)	0.348	0.426	0.452	0.167	0.247	0.285	0.260	0.302	0.307

2. – Framework for Wigner projection

The Wigner density functional formalism is based on the quantal density matrix projection, where the probability that a meson i is produced is given by $P_i = \mathrm{Tr}(\rho_i \rho^{(N)})$ with ρ_i being the density matrix of the meson i and $\rho^{(N)}$ the density matrix of the N heavy quarks and antiquarks produced in a pp collision. A partial Fourier transformation of the density matrices then yields

$$\frac{dP_i}{d^3\mathbf{R}d^3\mathbf{P}} = \sum \int \frac{d^3r d^3p}{(2\pi)^6} W_i(\mathbf{r},\mathbf{p}) \prod_{j>2} \int \frac{d^3r_j d^3p_j}{(2\pi)^{3(N-2)}} W^{(N)}(\mathbf{r}_1,\mathbf{p}_1,\mathbf{r}_2,\mathbf{p}_2,\ldots,\mathbf{r}_N,\mathbf{p}_N). \tag{1}$$

W_i is the two-body Wigner density of the bound heavy quark pair, and $W^{(N)}(\mathbf{r}_1,\mathbf{p}_1,\mathbf{r}_2,\mathbf{p}_2,...,\mathbf{r}_N,\mathbf{p}_N)$ is the quantal density matrix in Wigner representation of the ensemble of N heavy quarks produced in a pp collision. $\mathbf{r}(\mathbf{R})$ and $\mathbf{p}(\mathbf{P})$ are the relative (center of mass) coordinates and momenta of the heavy quark and antiquark bound in a quarkonium. We assume that the unknown quantal N-body Wigner density can be replaced by the average of classical phase space distributions, $W^{(N)} \approx \langle W^{(N)}_{\mathrm{classical}} \rangle$.

The classical momentum space distributions of the heavy quarks are provided by EPOS4 [5, 6]. However, EPOS4 only provides the coordinate information of the vertex where the $Q\bar{Q}$ pair is created. For a heavy quark pair created at the same vertex, we assume that the relative distance between Q and $\bar{Q}$ in their center-of-mass frame is given by a Gaussian distribution. The Wigner density for a $Q\bar{Q}$ pair can then be expressed as

$$W^{(2)}(\mathbf{r},\mathbf{p}) \sim r^2 \exp\left(-\frac{r^2}{2\sigma^2_{\mathrm{Q\bar{Q}}}}\right) f^{\mathrm{EPOS4}}_{\mathrm{Q\bar{Q}}}(\mathbf{p}), \tag{2}$$

where the distance is controlled by the effective width $\sigma_{\mathrm{Q\bar{Q}}}$. With the momenta and positions of the heavy quarks, we can calculate the yield of charmonium and bottomonium according to eq. (1).

Now we come to the construction of the Wigner density of the quarkonium. The Wigner density is obtained by the Wigner-Weyl transformation of the density matrix of the quarkonium.

The wave function of the quarkonium is the solution of the two-body Schrödinger equation, which we solve for charmonium and bottomonium with the Cornell potential, $V(r) = -\alpha/r + \kappa r + c$ with $\alpha = 0.513$, $\kappa = 0.17\mathrm{GeV}^2$, $c = -0.161$, and with the quark masses $m_c = 1.5\mathrm{GeV}$ and $m_b = 5.2\mathrm{GeV}$. The wave functions are shown in fig. 1, and the masses as well as the root-mean-square radii $\langle r^2\rangle$ are listed in table I. We observe that the masses are very close to the experimental values.

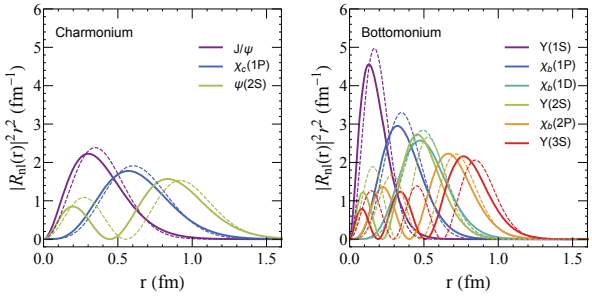

Fig. 1. – Wave function of different charmonium (left) and bottomonium (right) states. Solid lines are from the Schrödinger equation, dashed lines are from the 3-D isotropic harmonic oscillator (eq. (3)).

However, the wave function is not analytical, so the Wigner density can only be calculated numerically, which complicates the solution of eq. (1). It is therefore convenient to approximate the wave function by a 3D isotropic harmonic oscillator wave function for the potential $V(r) = 1/(2m_Q\sigma^4)r^2$. These wave functions are analytical and can be expressed as $\psi_{nlm}(r,\theta,\phi) = R_{nl}(r)Y_{l,m}(\theta,\phi)$, where $Y_{l,m}$ are the spherical harmonics.

The radial part can be expressed as follows:

$$R_{nl}(r) = \left[\frac{2(n!)}{\sigma^3\Gamma(n+l+3/2)}\right]^{\frac{1}{2}} \left(\frac{r}{\sigma}\right)^l e^{-\frac{r^2}{2\sigma^2}} L_n^{l+1/2}\left(\frac{r^2}{\sigma^2}\right), \tag{3}$$

where $L_n^{l+1/2}$ are Laguerre polynomials. The parameters of the 3-D isotropic harmonic oscillator wave functions are chosen to match the root-mean-square radius $\langle r^2\rangle$ of the real quarkonium wave function: $\langle r^2\rangle = 3\sigma^2/2$ for $1S$, $\langle r^2\rangle = 5\sigma^2/2$ for $1P$, $\langle r^2\rangle = 7\sigma^2/2$ for $1D$ and $2S$, $\langle r^2\rangle = 9\sigma^2/2$ for $2P$, and $\langle r^2\rangle = 11\sigma^2/2$ for $3S$ states. The corresponding widths are shown in table I and the wave functions are shown in fig. 1 with dashed lines. We can see that the ground states and low lying excited states can be well reproduced by the 3-D isotropic harmonic oscillator, while the difference increases for higher excited states, *e.g.* $2S$, $2P$, and $3S$.

With this analytical wavefunction, the Wigner function can be constructed via a Wigner transformation in the spherical coordinate. The Wigner function for any give (n,l) state can be expressed as

$$\begin{aligned} W_{nl}(\mathbf{r},\mathbf{p}) =& \frac{1}{2l+1}\frac{(-1)^l}{2\pi^3} \sum_{n'+N+l'=K} (-1)^{n'+3l'/2} \\ &\times \sqrt{\frac{\pi(2l+1)(2l'+1)n'!N!}{\Gamma(n'+l'+3/2)\Gamma(N+l'+3/2)}} \\ &\times (n'l'Nl'0|nlnl0) L_N^{l'+1/2}(2\mathbf{r}^2) L_N^{l'+1/2}(2\mathbf{p}^2) \\ &\times (2|\mathbf{r}||\mathbf{p}|)^{l'} P_{l'}(\cos\theta) e^{-(\mathbf{r}^2+\mathbf{p}^2)}, \end{aligned} \tag{4}$$

where $K = 2n+l$. θ is the angle between $\mathbf{r}$ and $\mathbf{p}$. L_n^l is generalized Laguerre polynomial. $P_{l'}$ is Legendre polynomial. This form is firstly given by ref. [8]. $(n'l'Nl'0|nlnl0)$ is Talmi-Brody-Moshinsky (TBM) brackets.

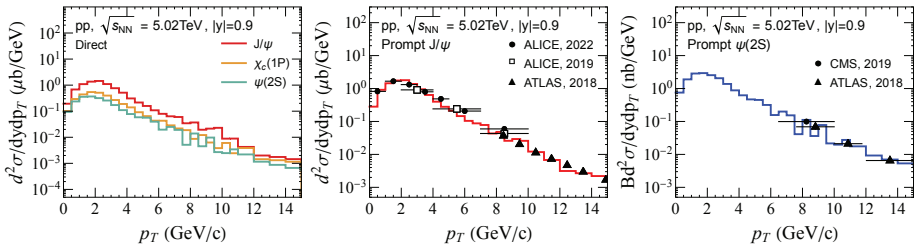

Fig. 2. – p_T spectra of different charmonium states (left), where red is J/ψ, orange is $\chi_c(1P)$, and green is $\psi(2S)$. Prompt J/ψ (middle). Prompt $\psi(2S)$ (right). The experimental data are from ALICE [9,10], ATLAS [11], and CMS [12].

The Wigner densities for different states up to $3S$ are

$$
\begin{aligned}
W_{1S}(\mathbf{r},\mathbf{p}) =& 8e^{-\xi},\\
W_{1P}(\mathbf{r},\mathbf{p}) =& \frac{8}{3}e^{-\xi}\Big(2\xi-3\Big),\\
W_{1D}(\mathbf{r},\mathbf{p}) =& \frac{8}{15}e^{-\xi}\Big(15+4\xi^2-20\xi+8[p^2r^2-(\mathbf{p}\cdot\mathbf{r})^2]\Big),\\
W_{2S}(\mathbf{r},\mathbf{p}) =& \frac{8}{3}e^{-\xi}\Big(3+2\xi^2-4\xi-8[p^2r^2-(\mathbf{p}\cdot\mathbf{r})^2)]\Big),\\
W_{2P}(\mathbf{r},\mathbf{p}) =& \frac{8}{15}e^{-\xi}\Big(-15+4\xi^3-22\xi^2+30\xi-8(2\xi-7)[p^2r^2-(\mathbf{p}\cdot\mathbf{r})^2]\Big),\\
W_{3S}(\mathbf{r},\mathbf{p}) =& \frac{8}{315}e^{-\xi}\Big(315+42\xi^4-336\xi^3+924\xi^2-840\xi-[2009+32p^2r^2\\
&+336r^4/\sigma^4-1400r^2/\sigma^2-896p^2\sigma^2+224p^4\sigma^4][p^2r^2-(\mathbf{p}\cdot\mathbf{r})^2]-[686\\
&+608p^2r^2+112r^2/\sigma^2-896p^2\sigma^2+224p^4\sigma^4-672(\mathbf{p}\cdot\mathbf{r})^2](\mathbf{p}\cdot\mathbf{r})^2\Big),
\end{aligned}
\tag{5}
$$

where $\xi=\frac{r^2}{\sigma^2}+p^2\sigma^2$. The transverse momentum and rapidity distribution of charmonium and bottomonium (see eq. (1)) are shown in figs. 2 and 3. We see, as far as data are available, a quite good agreement with the experimental results for $c\bar{c}$ as well $b\bar{b}$ mesons when choosing $\sigma_{c\bar{c}}=0.4$ fm and $\sigma_{b\bar{b}}=0.2$ fm in eq. (2).

We can conclude that the experimentally available rapidity and transverse momentum distribution of $c\bar{c}$ and $b\bar{b}$ quarkonia can be well described in the Wigner density formalism. The only parameter which enters the calculation is the width of the distribution of the relative distance of the $Q\bar{Q}$ pair at production. The relative contribution of the different states is then exclusively given by their wave function.

* * *

This work is funded by the European Union's Horizon 2020 research and innovation program under grant agreement No. 824093 (STRONG-2020). TS and EB acknowledge support by the Deutsche Forschungsgemeinschaft through the grant CRC-TR 211, Project N 315477589 - TRR 211.

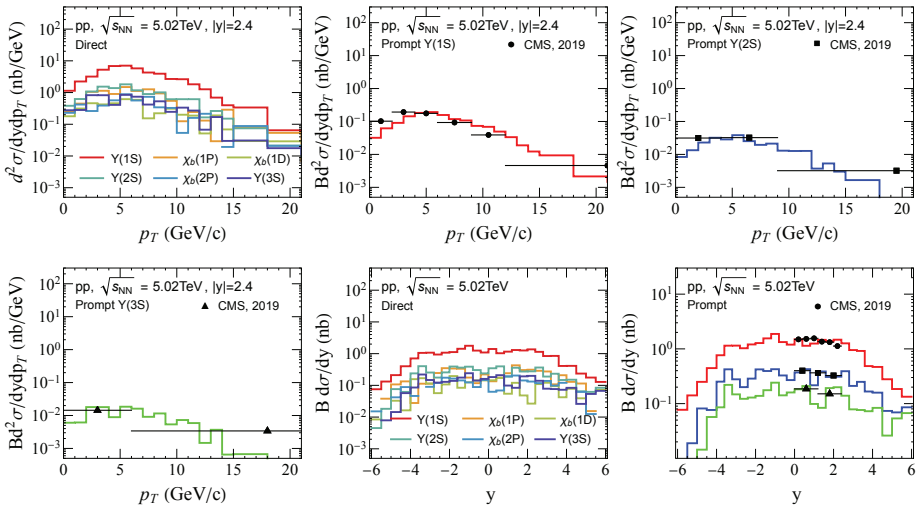

Fig. 3. – p_T and rapidity y dependence of different bottomonium states. The experimental data are from CMS [13].

REFERENCES

[1] Andronic A. *et al.*, *Eur. Phys. J. C*, **76** (2016) 107, arXiv:1506.03981.
[2] Song T., Aichelin J. and Bratkovskaya E., *Phys. Rev. C*, **96** (2017) 014907, arXiv:1705.00046.
[3] Villar D. Y. A., Zhao J., Aichelin J. and Gossiaux P. B., *Phys. Rev. C*, **107** (2023) 054913, arXiv:2206.01308.
[4] Song T., Aichelin J., Zhao J., Gossiaux P. B. and Bratkovskaya E., *Phys. Rev. C*, **108** (2023) 054908, arXiv:2305.10750.
[5] Werner K., *Phys. Rev. C*, **108** (2023) 064903, arXiv:2301.12517.
[6] Werner K. and Guiot B., *Phys. Rev. C*, **108** (2023) 034904, arXiv:2306.02396.
[7] Particle Data Group Collaboration (Workman R. L. *et al.*), *PTEP*, **2022** (2022) 083C01.
[8] Shlomo S. and Prakash M., *Nucl. Phys. A*, **357** (1981) 157.
[9] ALICE Collaboration (Acharya S. *et al.*), *JHEP*, **03** (2022) 190, arXiv:2108.02523.
[10] ALICE Collaboration (Acharya S. *et al.*), *JHEP*, **10** (2019) 084, arXiv:1905.07211.
[11] ATLAS Collaboration (Aaboud M. *et al.*), *Eur. Phys. J. C*, **78** (2018) 171, arXiv:1709.03089.
[12] CMS Collaboration (Sirunyan A. M. *et al.*), *Phys. Lett. B*, **790** (2019) 509, arXiv:1805.02248.
[13] CMS Collaboration (Sirunyan A. M. *et al.*), *Phys. Lett. B*, **790** (2019) 270, arXiv:1805.09215.